

Supporting Information

Synergism of Dewetting and Self-Wrinkling to Create Two-Dimensional Ordered Arrays of Functional Microspheres

Xue Han,[†] Jing Hou,[†] Jixun Xie,[†] Jian Yin,[†] Yi Tong,[†] Conghua Lu^{†} and Helmuth Möhwald[‡]*

[†]School of Materials Science and Engineering, Tianjin University, Tianjin, 300072, P. R. China

[‡]Department of Interfaces, Max Planck Institute of Colloids and Interfaces, Potsdam, 14424, Germany

Corresponding Author

*Address correspondence to chlu@tju.edu.cn.

1 Supplementary Figures and Discussions

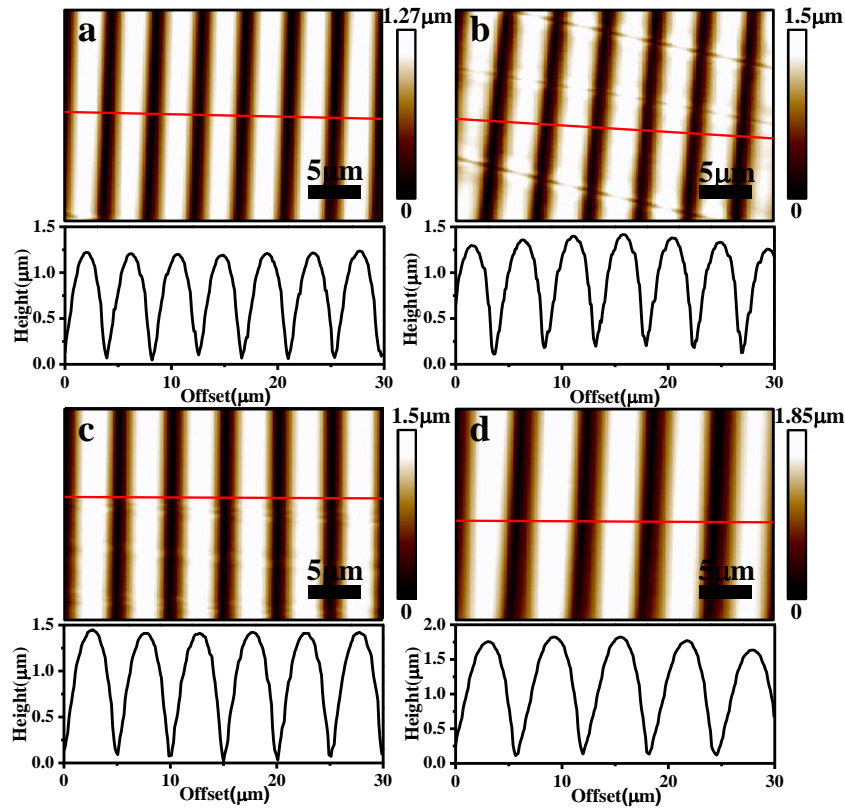


Figure S1. AFM height images and corresponding cross-section profiles of the wrinkled PDMS templates with different wavelengths (λ_t) and amplitudes (A_t) applied for the wrinkle-directed dewetting. $\lambda_t/A_t =$ (a) $4.2 \mu\text{m}/1.2 \mu\text{m}$; (b) $4.5 \mu\text{m}/1.3 \mu\text{m}$; (c) $4.8 \mu\text{m}/1.4 \mu\text{m}$; (d) $6.3 \mu\text{m}/1.8 \mu\text{m}$.

The wrinkled PDMS template with well-oriented sinusoidal profiles was prepared by oxygen plasma (OP) exposure of an uniaxially strained PDMS sheet, followed by slow relief of the pre-strain. It is well accepted, that OP exposure leads to the conversion of the PDMS surface into a rigid silica-like (SiO_x) layer.^{1,2} In the process of slow release of the uniaxial pre-strain, the compressive strain, which is parallel to the pre-strain, is generated on the as-formed SiO_x layer due to the moduli mismatch

between the top oxidized SiO_x layer and the underlying compliant PDMS substrate. Once the compressive strain ε exceeds the critical wrinkling strain ε_c , namely $\varepsilon > \varepsilon_c$, surface wrinkles with the orientation orthogonal to the compressive strain (*i.e.*, the pre-strain direction) are induced into the sinusoidal profiles. Based on the following Equations 1 and 2 the wavelength (λ) and amplitude (A) of the oriented wrinkles can be well tuned by the film thickness.^{3,4}

$$\lambda = 2\pi h \left(\frac{\bar{E}_f}{3\bar{E}_s} \right)^{\frac{1}{3}} \quad (1)$$

$$A = h \left(\frac{\varepsilon - \varepsilon_c}{\varepsilon_c} \right)^{\frac{1}{2}} \quad (2)$$

where h is the film thickness, $\bar{E} = E/(1-\nu^2)$ is the plane-strain modulus (E is the elastic modulus, ν is the Poisson's ratio), and the subscripts f and s denote the film and the substrate, respectively.

In our experiment, the thickness of the oxidized SiO_x layer is conveniently manipulated by the OP exposure duration. Thus, the required wrinkled PDMS templates with different wavelengths (λ_t) and amplitudes (A_t) can be easily fabricated by selecting proper OP exposure duration.

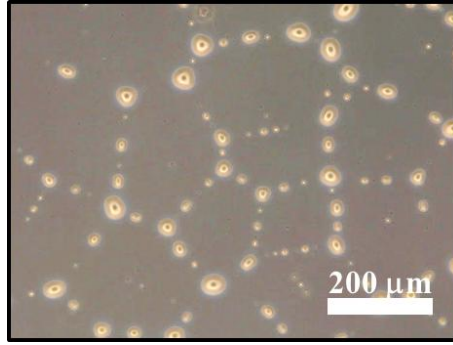


Figure S2. The planar PEG/PS/PDMS trilayer after sequentially spin-coating of PS and PEG onto the OP-activated PDMS substrate.

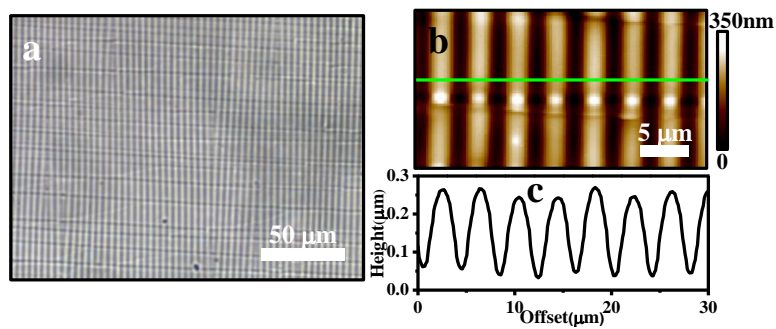


Figure S3. Optical microscope (a), AFM height (b) images, and the corresponding cross-section profile (c) of the planar PEG/PS/PDMS trilayer after the wrinkle-directed dewetting, followed by final water washing.

Section S1. Calculation of the compressive stress σ exerted on the PS/PDMS bilayer and of the required critical wrinkling stress σ_c .

When the temperature is decreased from 95 °C to 80 °C, the compressive stress σ exerted on the PS/PDMS bilayer can be estimated according to Equation 3:³

$$\sigma = \frac{E_f(\alpha_s - \alpha_f)(T_1 - T_2)}{(1 - \nu_f)}. \quad (3)$$

On the other hand, the critical wrinkling stress σ_c required for surface wrinkling on a PS/PDMS bilayer is given by^{3,5}

$$\sigma_c = \frac{E_f}{4(1 - \nu_f^2)} \left(\frac{3E_s(1 - \nu_f^2)}{E_f(1 - \nu_s^2)} \right)^{\frac{2}{3}} \quad (4)$$

Here assuming that $E_f = 3.4$ GPa, $\nu_f = 0.33$, $\alpha_f = 8 \times 10^{-5}$ °C⁻¹, $E_s = 1.5$ MPa, $\nu_s = 0.5$, $\alpha_s = 8.50 \times 10^{-4}$ °C⁻¹, $T_1 = 95$ °C, $T_2 = 80$ °C, then $\sigma = 58.61$ MPa, $\sigma_c = 12.90$ MPa.

Evidently, $\sigma > \sigma_c$, and thus surface wrinkling can be induced spontaneously on the PS/PDMS bilayer, when the 95 °C-heated bilayer is cooled to 80 °C.

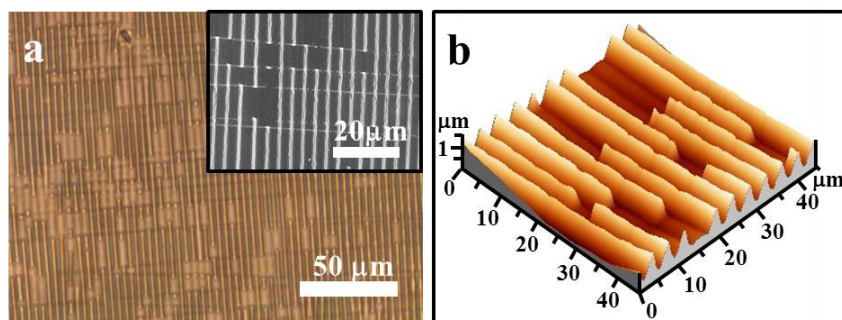


Figure S4. Optical microscope (a) and corresponding AFM 3D (b) images of the wrinkle-directed dewetted PEG/PS/PDMS trilayer after the wrinkled template was removed at room temperature. Inset in (a) is the corresponding SEM image.

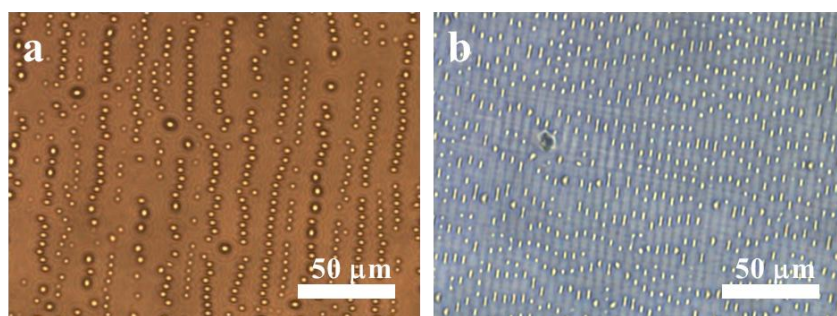


Figure S5. (a) PEG/PS/glass slide trilayer after wrinkle-directed dewetting. (b) After removing the wrinkled PDMS template at 80 °C, the dewetted PEG/PS/PDMS trilayer was quickly cooled to room temperature.

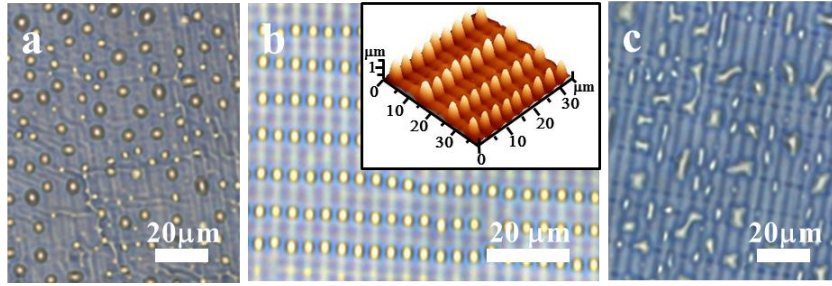


Figure S6. Influences of C_{PS} and C_{PEG} on the wrinkle-directed dewetting patterns: (a) $C_{PS} = 1$ wt%, $C_{PEG} = 2$ wt%; (b) $C_{PS} = 3$ wt%, $C_{PEG} = 2$ wt%; (c) $C_{PS} = 2$ wt%, $C_{PEG} = 4$ wt%.

Figure S6 shows that the 2-D ordered PEG microsphere arrays are strongly dependent on C_{PS} and C_{PEG} . For instance, when C_{PEG} is fixed to be 2 wt%, ordered PEG microsphere arrays are successfully formed on the crests of *in-situ* wrinkles with $C_{PS} = 2$ wt% and 3wt% applied, while the dewetted PEG microspheres completely lose the order and regularity with $C_{PS} = 1$ wt% (Figures 2b-d and S6a,b). Too low C_{PS} with much thinner PS film leads to a smaller λ_i , which inevitably makes $r = \lambda_i/\lambda_i$ become larger. This too large r eventually fails to effectively confine the surface wrinkling along the contour of the imposed wrinkled PDMS template, and then randomly oriented wrinkles are observed on the PS/PDMS bilayer. At this point, the dewetting of top PEG is disturbed by these random wrinkles and finally evolves into chaotically distributed PEG microspheres (Figure S6a). On the other hand, when C_{PS} is kept to be 2 wt%, irregular PEG debris lies on the *in-situ* striped wrinkles with $C_{PEG} = 4$ wt% applied (Figure S6c). In this case, PEG is so abundant, that the overflow from the crests of *in-situ* wrinkles to the valleys happens, and then irregular PEG dewetting results. This suggests that the *in-situ* formed striped wrinkles cannot accommodate the

high concentration of PEG for the directed dewetting. The dependence of the dewetting patterns on C_{PS} and C_{PEG} effectively indicates the vital role of the cooperation of the wrinkled template and the *in-situ* self-wrinkling substrate. It is noticeable that λ_t , C_{PS} and C_{PEG} are dominant variables for the morphology manipulation. We can not only tune the sizes and adjacent spacing of the arrayed PEG microspheres, but also adjust the single or double lined arrays of the dewetted microspheres, which has been inaccessible to other methods so far.

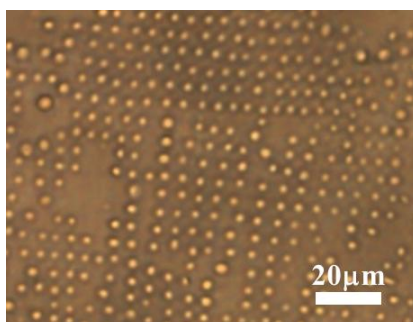


Figure S7. Optical microscope image of the ordered PEG microsphere arrays on a glass slide transferred from the wrinkled PS/PDMS bilayer.

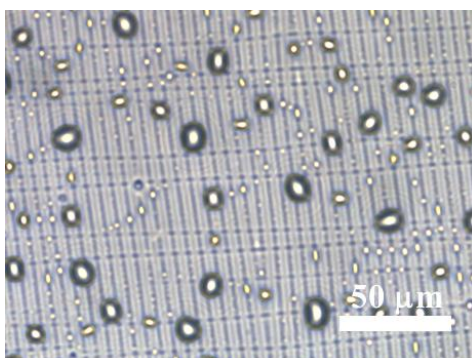


Figure S8. Optical microscope image of the wrinkled PS/PDMS bilayer after confinement-induced surface wrinkling, followed by spin-coating of a PEG solution.

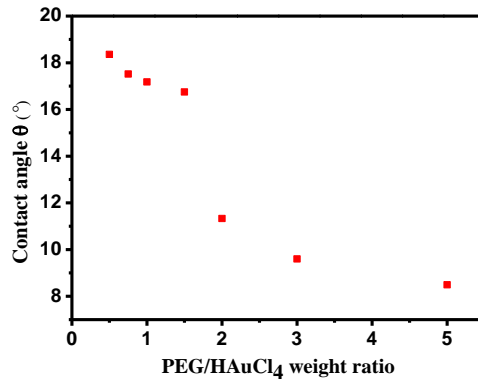


Figure S9. Relation of contact angles θ of the PEG-HAuCl₄ mixed solution on the planar PS/PDMS bilayer with the weight ratio of PEG/HAuCl₄.

The dewetting behavior of PEG-HAuCl₄ mixed solution on the planar PS/PDMS bilayer surface is investigated. Contact angle measurements show, that the contact angle of PEG-HAuCl₄ mixed solution on the PS film increases slowly from 5.8° (PEG solution in the absence of HAuCl₄) to 11.3°, when the weight ratio of PEG/HAuCl₄ decreases to 2. Further decreasing the weight ratio to 1.5 leads to an abrupt increase of the contact angle θ to 16.7°, and hereafter a small contact angle increase appears. This change in the contact angle is believed to be connected with the association between HAuCl₄ and PEG, simultaneously implying that the PEG-HAuCl₄ composite is more polar and thus more prone to dewet on the PS film than pure PEG. In the following experiment, the wrinkle-directed dewetting on the (PEG-HAuCl₄)/PS/PDMS trilayer is systematically investigated, while the weight ratio of PEG/HAuCl₄ is fixed to be 1.5, considering their relatively large contact angle on the PS film favoring dewetting.

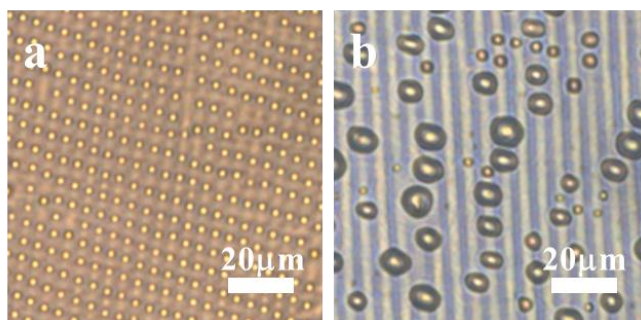


Figure S10. Influence of C_{PEG} on the wrinkle-directed dewetting patterns on the (PEG-HAuCl₄)/PS/PDMS trilayer. $C_{\text{PEG}} = 2$ wt% (a); 4 wt% (b).

Highly ordered 2-D PEG-HAuCl₄ composite microsphere arrays on the *in-situ* wrinkles have been fabricated with $C_{\text{PEG}} = 2$ or 3 wt% (Figures 5a-d and S10a). When $C_{\text{PEG}} = 4$ wt%, the *in-situ* formed striped wrinkles could not accommodate the high concentration of PEG for the directed dewetting, so irregular composite microspheres with different diameters spread on these *in-situ* striped wrinkles (Figure S10b).

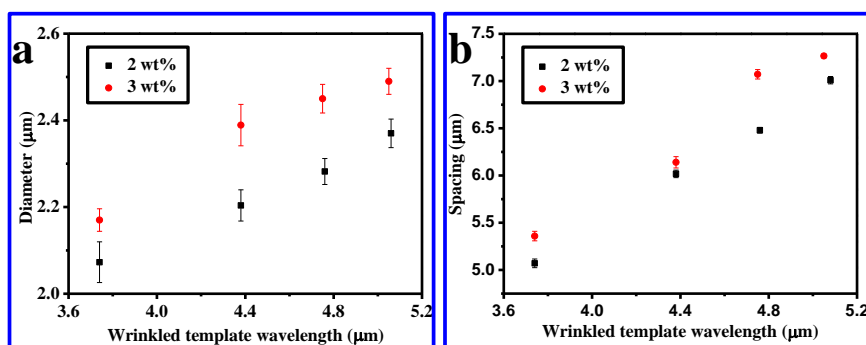


Figure S11. Dependence of the diameters (a) and spacing (b) of dewetted PEG-HAuCl₄ composite microspheres on the wrinkled template wavelengths λ_t in the case of $C_{\text{PEG}} = 2$ wt% and $C_{\text{PEG}} = 3$ wt% applied, respectively. The diameters and spacings of the composite microspheres are still almost linear to λ_t , which is consistent with the results of PEG microspheres observed in Figure 3e,f.

Section S2. The as-formed highly ordered 2-D arrays of PEG-HAuCl₄ composite microspheres exclusively isolated on the *in-situ* wrinkled PS/PDMS bilayer were controllably converted into the corresponding periodically aligned Au nanoparticle arrays via different reduction approaches.

Firstly, the PEG-HAuCl₄ composite microsphere arrays were subjected to OP exposure. OP could not only reduce the HAuCl₄ salts into Au nanoparticles, but also remove the existing polymers, such as PEG and PS. After OP exposure for 60 min, periodically ordered Au nanoparticle arrays were successfully fabricated (Figure 5e). Meanwhile, the *in-situ* striped PS wrinkles disappear, demonstrating that PEG and PS have been removed (Figure 5e). When ordered PEG-HAuCl₄ composite microsphere arrays were treated by N₂H₄ vapor, followed by OP exposure, an Au nanoparticle array with eye-like morphologies is obtained (inset of Figure 5f). It is well accepted, that N₂H₄ vapor can completely reduce HAuCl₄ salts without damaging the coordinated PEG chains.⁶ These HAuCl₄ salts are regarded as uniform distribution in each composite microsphere, on account of the coordination with PEG backbone chains. Once the reduction happened, the complexation between HAuCl₄ and PEG chains, namely the binding force, would be weakened and damaged. Partially hydrophobic Au nanoparticles can migrate to the edge of the microspheres and act as a surfactant to reduce the interfacial tension between the substrate and the PEG microspheres. However, the microsphere diameter is so large, that only part of the nanoparticles near the edge have enough time to move to the edge to form a ring, and

those far away from the edge are left in the center of the microspheres. Subsequent OP treatment further removes the polymers of PEG and eye-like morphologies of Au nanoparticle arrays were obtained. Thus it can be seen, that different reduction approaches can lead to different arrayed Au nanoparticle morphologies, which could be flexibly applicable in different fields.

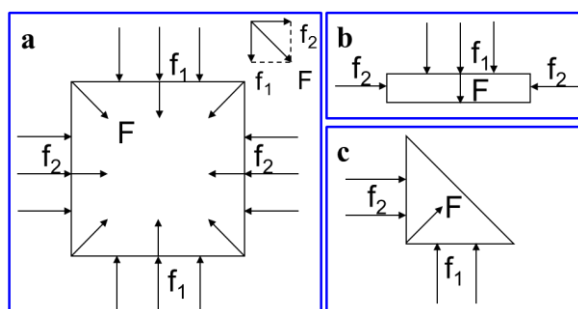


Figure S12. (a) Sketch of the forces in different regions of the samples. F is the resultant force of components f_1 (parallel to the wrinkle direction) and f_2 (perpendicular to the wrinkle direction). Different shapes of the wrinkled templates, such as rectangular (b) and right-angled triangular (c) ones, could be employed subsequently.

2 Supplementary References

1. Bayley, F. A.; Liao, J. L.; Stavrinou, P. N.; Chiche, A.; Cabral, J. T. Wavefront Kinetics of Plasma Oxidation of Polydimethylsiloxane: Limits for Sub-um Wrinkling. *Soft Matter* **2014**, *10*, 1155-1166.
2. Han, X.; Zhao, Y.; Cao, Y.; Lu, C. Controlling and Prevention of Surface Wrinkling via Size-Dependent Critical Wrinkling Strain. *Soft Matter* **2015**, *11*, 4444-4452.
3. Bowden, N.; Brittain, S.; Evans, A. G.; Hutchinson, J. W.; Whitesides, G. M. Spontaneous Formation of Ordered Structures in Thin Films of Metals Supported on an Elastomeric Polymer. *Nature* **1998**, *393*, 146-149.
4. Genzer, J.; Groenewold, J. Soft Matter with Hard Skin: From Skin Wrinkles to Templating and Material Characterization. *Soft Matter* **2006**, *2*, 310-323.
5. Mei, H.; Huang, R.; Chung, J. Y.; Stafford, C. M.; Yu, H.-H. Buckling Modes of Elastic Thin Films on Elastic Substrates. *Appl. Phys. Lett.* **2007**, *90*, 151902.
6. Park, M.; Hyun, D. C.; Kim, J.; Kim, Y. S.; Jeong, U. Dewetting-Induced Formation of Periodic Dot Arrays of Polymer/Au Composites by Capillary Force Lithography. *Chem. Mater.* **2010**, *22*, 4166-4174.